Sulfonated Multiwalled Carbon Nanotube/Sulfonated Poly(Ether Sulfone) Composite Membrane with Low Methanol Permeability for Direct Methanol Fuel Cells

Sungjin Yun, Yusun Heo, Hyungu Im, Jooheon Kim

School of Chemical Engineering & Material Science, Chung-Ang University, Heukseok-Dong, Dongjak-Gu, Seoul 156-756, Korea

Received 11 July 2011; accepted 4 January 2012
DOI 10.1002/app.36741
Published online in Wiley Online Library (wileyonlinelibrary.com).

ABSTRACT: An organic/inorganic composite membrane was prepared based on sulfonated poly(ether sulfone) (s-PES) embedded with sulfonated multiwalled carbon nanotubes (s-MWNTs). The ion exchange capacity (IEC), proton conductivity, and water uptake of the SPES membranes increased with increasing s-MWNTs content. The increased water uptake was attributed to hydrogen bond formation between the carbonyl group of the s-MWNTs and a water molecule. The composite membranes exhibited proton conductivities ranging from 3.9281×10^{-4} to 7.0788×10^{-3} S/cm at 80°C, as well as low methanol permeability ranging from 4.4405×10^{-10} to 9.1008×10^{-10} $cm^2\ s^{-1}$ at 25°C. © 2012 Wiley Periodicals, Inc. J Appl Polym Sci 000: 000–000, 2012

Key words: fuel cell; direct methanol fuel cell; poly(ether sulfone); multiwalled carbon nanotube; methanol permeability

INTRODUCTION

Direct membrane fuel cells (DMFCs) have attracted considerable attention as a fuel cell technology because they have stable operation, high energy efficiency and are a portable power source with low environmental pollution.[1–4] The polymer electrolyte membrane (PEM), which transfers protons from the anode and cathode, is one of the most critical components in a DMFC. The PEM should have low reactant (methanol) and oxidant permeability.[5–9] Currently, Nafion®, a perfluorinated sulfonic ionomer, is the major membrane used in DMFCs owing to its high proton conductivity and chemical stability when hydrated.[10,11] On the other hand, Nafion® is expensive and is associated with high methanol crossover, which decreases the fuel cell efficiency.[12–14]

Recent research has focused on developing a Nafion® replacement to overcome the established drawbacks of the PEM.[15] Na et al.[1] prepared novel cross-linked sulfonated poly(arylene ether ketone) membranes with higher proton conductivity and lower methanol crossover than Nafion®. Kim et al.[16] synthesized cross-linked poly(ether ether ketone) membranes with much lower methanol permeability than Nafion®. Other alternative membranes include polyethyleneimine, polyethersulfone (PES), polybenzimibazole, and polyvinylalcohol.

Sulfonated aromatic polymers have been examined as alternatives to Nafion® owing to their low cost, good physical properties, and high proton conductivity. Among these aromatic polymers, PES membranes have attracted attention for their good physical properties and chemical stability.[17–19] In previous studies, PES membranes were subdivided into two major categories. First, they were mixed with other polymers to improve the proton conductivity and mechanical properties. Lee et al.[20] reported sulfonated poly(arylene ether sulfone)/poly(ether sulfone) (s-PES) semi-IPN membranes, and Shu et al.[21] synthesized a sulfonated poly(ether imide)/s-PES composite membrane. In the second case, inorganic fillers were introduced into the PES matrix because they can improve the improve physical and chemical properties of interest (such as elastic modulus, proton conductivity, solvent permeation rate, tensile strength, hydrophilicity, and glass-transition temperature).[19,22,23] Prashantha et al.[22] used titanium dioxide particles in a PES matrix to show that an inorganic oxide network decreases the methanol permeability. In another study, Sheng et al.[19] reported that PES/silica composite membranes have higher selectivity (the ratio of proton conductivity to methanol permeability) than Nafion 112.

Carbon nanotubes (CNTs) have attracted considerable attention for their role in the development of multifunctional nanocomposite materials. Compared

Correspondence to: J. Kim (jooheonkim@cau.ac.kr).

with nanocomposites filled with inorganic fillers as conducting reinforcements, polymeric nanocomposites with multiwalled carbon nanotubes (MWNTs) can form a conducting pathway at relatively very low concentrations due to their high aspect ratios of 100–1000 and high specific surface areas.[24–31] Because of these unique properties, in recent years, MWNTs have been widely investigated as candidate PEM materials. Choi et al.[32] reported on a membrane of blended functionalized carbon nanotubes (CNTs) and sulfonated poly(arylene sulfone) (sPAS) for use in a direct methanol fuel cell. Furthermore, Thomassin et al.[33] prepared a MWNT/Nafion membrane to decrease the methanol crossover. Although CNTs possess these excellent properties, they are difficult to disperse in solvents and tend to agglomerate, forming granules of various sizes, which can affect the electrical conductivity.[34,35]

This article reports a novel PES membrane that was prepared using sulfonated MWNTs (s-MWNTs) and s-PES. The effect of the s-MWNTs/s-PES (SPES) composite membranes on the proton conductivity was examined. The SPES composite membranes were also examined to determine the membrane properties, including water uptake, mechanical properties, and methanol permeability.

MATERIALS

The MWNTs (diameter, 20–30 nm; >99% purity) used in this study were supplied by Hanhwa Nano Tech (Seoul, Korea). Nitric acid (HNO_3, HPLC grade, Aldrich, Seoul), sulfuric acid (H_2SO_4, HPLC grade, Samchun Chemical, Pyungteak, Korea), and thionyl chloride ($SOCl_2$, Samchun Chemical, Pyungteak, Korea) were used as received. PES (Aldrich, Seoul), N,N-dimethylformamide (DMF, Aldrich, Seoul), methanol (MeOH, HPLC grade, Aldrich, Seoul), deionized water (DI water, HPLC grade, Aldrich, Seoul), sodium chloride (NaCl, Aldrich, Seoul), and phenolphthalein (PH indicator) were purchased from Sigma Chemical. Aminomethanesulfonic acid (TCI, Tokyo, Japan) was also used as received.

Synthesis of s-PES

PES was sulfonated by following the method described earlier.[36] s-PES was made by dissolving an PES powder (10 g) in 250 mL of H_2SO_4 (95–98%). This mixture was reacted under mechanical stirring at 50°C for 48 h. The reacted mixture was dropped gradually into an ice bath (DI water) with constant stirring, and the obtained polymer was filtered through a 450 nm nylon membrane. The s-PES powder was finally washed with DI water until the pH was neutral and overnight to remove the residual sulfuric acid. The s-PES powder was dried for 4 h in a vacuum oven at 50°C. Figure 1 gives a schematic diagram of the sulfonation process of the PES matrix.

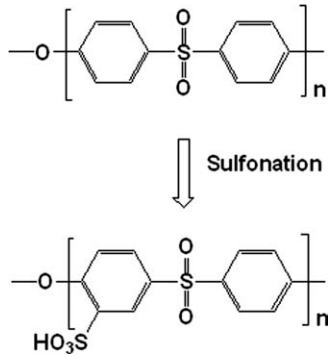

Figure 1 Sulfonation of PES polymer.

Synthesis of the functionalized MWNTs (s-MWNTs)

The pristine MWNTs (0.2 g) were mixed into a solution of 98% H_2SO_4 (80 mL) and 70% HNO_3 (20 mL) with constant stirring under reflux. The amount of raw MWNTs in the acid solution mixture was approximately 0.0025 wt %. The reactant was placed on a hot plate, stirred, and heated to 50°C for 24 h. After chemical oxidation, the treated MWNTs were separated from the acids by filtration, washed thoroughly with DI water, and dried at 100°C. The resulting acid treated MWNTs powders were dispersed in a $SOCl_2$ solution (250 mL) with sonication for 2 h and stirred for 12 h at 60°C. The suspension was vacuum-filtered through a 450 nm PTFE membrane and dried for 12 h under vacuum at ambient temperatures. Aminomethanesulfonic acid (2 g) was dissolved in 250 mL of deionized water followed by the addition of MWNTs-COCl powders. This mixture was reacted by mechanical stirring at 80°C for 24 h. The resulting solution was filtered through a 450 nm nylon membrane and dried at 100°C. Figure 2 gives a schematic diagram of the sulfonation of MWNTs.

Preparation of SPES composite membranes

s-PES in DMF (10%, 20 mL) was mixed with various s-MWNTs contents (0%, 1%, 2%, 3%, and 5%) and stirred at room temperature for 1 day followed by sonicating for 2 h to obtain a s-PES/s-MWNTs solution. All SPES mixture solutions were cast on Petri dishes and heated to 100°C for 12 h. The fabricated SPES membranes were peeled off the dishes and dried in a vacuum at 60°C for 12 h. The thickness of the SPES membranes ranged from 100 μm and 120 μm.

Characterization

Fourier transform infrared

Fourier transform infrared (FT-IR, Bio-rad FTS-165, Thermo Fisher Scientific, USA) spectroscopy was

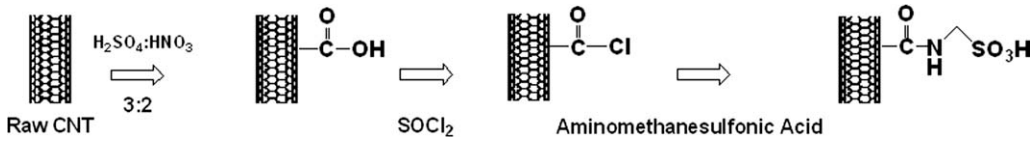

Figure 2 Sulfonation of s-MWNTs.

performed to examine the changes in the functional groups of s-PES. The FT-IR spectra were collected after 32 scans in the 4000–500 cm^{-1} region in attenuated total reflection (ATR) mode at a resolution of 4 cm^{-1}.

^{1}H-NMR

The characterization of s-PES was performed by measuring the degree of sulfonation (DS) using ^{1}H-NMR spectroscopy (Gemini 2000, Verian) at a resonance frequency of 300 MHz with DMSO-d6 as the solvent and tetramethyldilane as the reference standard.

Thermogravimetric analysis

Thermogravimetric analysis (TGA, TGA-2050, TA instruments) was performed from room temperature to 800°C at a heating rate 10°C min^{-1}.

Scanning electron microscopy

The microstructural transformation of the s-MWNTs and SPES nanocomposite membranes was analyzed by high resolution scanning electron microscopy (SEM, S-4300SE, Hitachi). The SPES films were fractured in liquid nitrogen, and these samples were sputter coated with Pt before to the SEM measurements.

Mechanical property

The tensile tests were carried out using an Instron 5565A universal testing machine at room temperature. The films were prepared into dog-bone specimens with dimensions of 3.82 mm × 1.57 mm × 1.24 mm. The tensile strength of the films was measured with a gauge length of 20 mm and a crosshead speed of 1.3 mm/min.

Ion exchange capacity

The ion exchange capacity (IEC) of the SPES membranes was measured by titration. Dry SPES membranes were immersed in 1 mol of a NaCl solution for 24 h to replace all the H^+ with Na^+. The amount of H^+ protons released from the membranes was determined by titration using a 0.01 M NaOH solution with phenolphthalein as the pH indicator. The IEC value was obtained using the following equation[9]:

$$\text{IEC} = \frac{\text{consumed NaOH (ml)} \times \text{molarity of NaOH}}{\text{weight of dried membrane}} \times (\text{mequiv g}^{-1}) \quad (1)$$

In addition to titration, ^{1}H-NMR spectroscopy can be used to determine both the DS and the IEC. The DS is defined as the average number of sulfonated groups per repeat unit. The DS value was calculated from ^{1}H-NMR spectroscopy.[39]

Water uptake

The SPES membranes were dried at 80°C under vacuum for 12 h, and the weight of the dried membranes was measured. The membranes were immersed in deionized water at different temperatures (25°C, 60°C, and 80°C). After 24 h, the surface solution of the wetted membranes was removed with tissue paper before weighing. The wetted membranes were then reweighed. The uptake was calculated using the following equation[29]:

$$\text{Water(or MeOH)uptake } (\%) = \frac{w_{\text{wet}} - w_{\text{dry}}}{w_{\text{dry}}} \times 100 \quad (2)$$

where w_{dry} and w_{wet} were the masses of dried and wet samples, respectively.

Methanol permeability

The methanol permeability of the SPES membranes was measured using a glass diffusion cell, consisting of two reservoirs each with a capacity of 100 mL. Before each test, the membranes were prehydrated for at least 24 h. Each reservoir was separated by a prehydrated membrane. One of the reservoirs contained 10 *M* methanol solution, whereas the other reservoir contained distilled deionized water. Both compartments were stirred continuously with a magnetic stirrer during the permeability experiment. The concentration of methanol in the water reservoir was measured by gas chromatography. The methanol permeability was calculated using the following equation[30]:

$$C_B(t) = \frac{A}{V_B}\frac{DK}{L}C_A(t - t_0) \quad (3)$$

where C_A and C_B are the concentrations of methanol in the donor and receptor reservoirs, respectively.

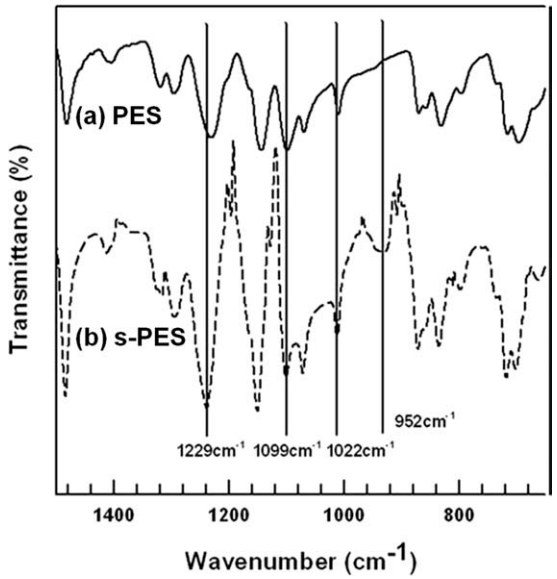

Figure 3 FT-IR spectra of (a) pure PES and (b) s-PES.

A and *L* are the diffusion area and thickness of the membrane, respectively. *D* and *K* are the methanol diffusivity and partition coefficient, respectively. The product of *DK* is the methanol permeability ($cm^2\ s^{-1}$).

Proton conductivity

The proton conductivity of the SPES membranes was measured by AC impedance spectroscopy using an IM-6ex, Zahner which facility can measured in range 10^{-12}–10^4 A (ampere) based on voltage from 0 to 10 V. Before the conductivity experiments, all samples were immersed in deionized water for at least 24 h at room temperature. The samples were sandwiched rapidly between two Pt electrodes. The electroconductivity (σ) of all samples was measured using a two-point method at different temperatures (25°C, 60°C, and 80°C). The electroconductivity (σ) was calculated using the following equation[30]:

$$\sigma = \frac{h}{(R \cdot S)} \tag{4}$$

where *h* is the thickness of the conducting membranes, *R* (Ω) is the electroresistance, and *S* (m^2) is the surface dimension of the membranes.

RESULTS

ATR-FT-IR spectra analysis

The effectiveness of sulfonation was examined by ATR-FT-IR. Figure 3(a,b) shows the spectra of the pure PES and s-PES, respectively. Both pure PES and s-PES displayed the typical absorption bands at 1229 cm^{-1}, 1099 cm^{-1}, and 1022 cm^{-1}. The characteristic absorption band for aryl oxide appeared at 1229 cm^{-1}. Two absorption peaks at 1099 cm^{-1} and 1022 cm^{-1} are characteristic of the aromatic SO_3^- stretching vibrations. One new peak of the s-PES appeared at approximately 952 cm^{-1}, which was assigned to the sulfonic acid group (—SO_3H). This suggests that the sulfonic acid groups had been reacted successfully in the PES molecules.

Confirmation of sulfonation process

In the ^{1}H-NMR spectra, confirmation on the presence of sulfonic acid groups in s-PES is based on the downfield shift from 7.24 ppm to 8.31 ppm of the hydrogen (H_E) located in the ortho position in the aromatic ring, as shown in Figure 4.

The DS was also determined by ^{1}H-NMR spectroscopy and titration. The ^{1}H-NMR method involves an analysis of the peak area of the H_E (AH_E) and the peak area of all other signals ($\sum H_{A,\ A1,\ B,\ B1,\ C,\ D}$). The DS can be obtained using the following expression[38]:

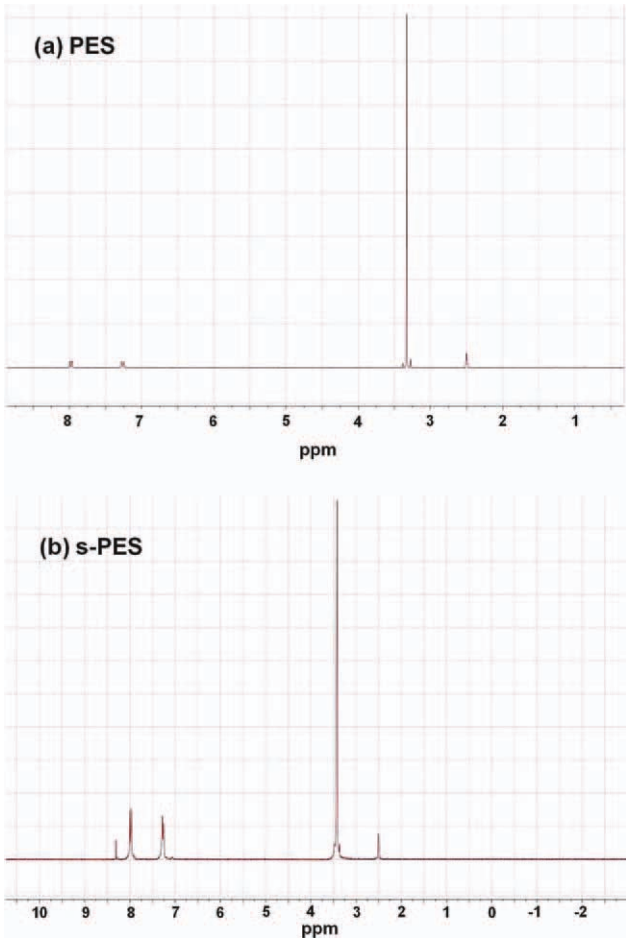

Figure 4 ^{1}H-NMR spectra of (a) PES and (b) s-PES. [Color figure can be viewed in the online issue, which is available at wileyonlinelibrary.com.]

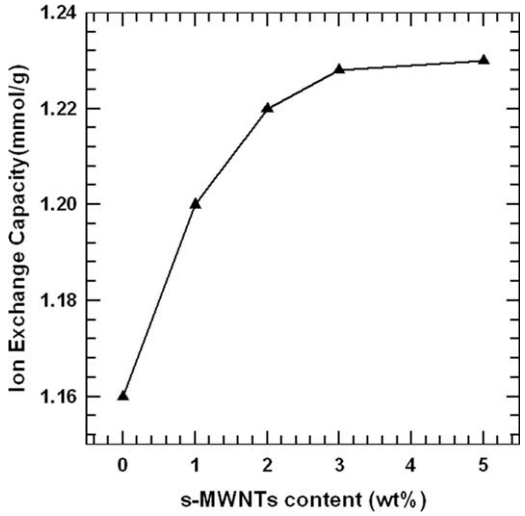

Figure 5 IEC values of SPES membranes at room temperature.

$$\frac{\mathrm{DS}}{(8-2\mathrm{DS})}=\frac{\mathrm{AH}_E}{\sum \mathrm{AH}_{A,A^1,B,B^1,C,D}} \tag{5}$$

The IEC of s-PES was obtained from DS using the following equation[38]:

$$\mathrm{IEC}=\frac{1000\mathrm{DS}}{232+81\times \mathrm{DS}} \tag{6}$$

The IEC of SPES was determined by a titration method (^{1}H-NMR method) and the results are shown in Figure 5. The IEC values of the SPES membranes increased from 0.8 up to 1.7 mequiv. g^{-1} with increasing s-MWNT weight ratio in the SPES membrane. The IEC of sulfonated PES is 0.62 mequiv. g^{-1}.[38] The increase in the measured IEC was attributed mainly to the addition of s-MWNTs, which contained many sulfonated groups. The analyses by ^{1}H-NMR (IEC = 1.08) and titration corresponded well.

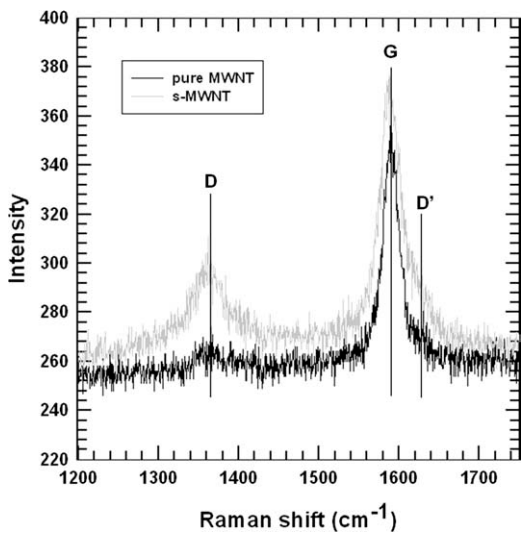

Figure 6 Raman spectra of pristine MWNTs and s-MWNTs.

Raman spectroscopy

Raman spectroscopy is widely used to characterize the functionalized MWNTs. In Raman spectra, we observe the peak of the G-band at 1585 cm^{-1}, which is assigned to the stretching of the C—C bond, and the peak of the D-band at 1359 cm^{-1}, originating from defects and disorder in the graphitic structure. As shown in Figure 6, the I_D/I_G peak intensity ratios of functionalized MWNTs exceeded those of pure MWNTs, which provides direct evidence of the modification of MWNT. The D-band intensity was increased in functionalized MWNTs compared with pure MWNTs. This indicates that the amount of defects of MWNTs are increased, which is attributed to the functionalization of the carboxyl groups and sulfonic groups in MWNT. In addition, the D′-band at 1620 cm^{-1}, which is affected by the disorder in nanotubes, is also present with different intensities for pure and functionalized MWNTs. Because the D′-band is not observed in pure MWNTs but is clearly detectable after functionalization, the D′-band in functionalized MWNTs is also evidence of increased defects (the sites functionalized in MWNT) in s-MWNTs.

SEM and EDX analysis

Figure 7 shows SEM images of the morphology of pristine-MWNTs and functionalized MWNTs. A comparison of the morphology of pristine MWNTs (a) with that of functionalized MWNTs (b) showed

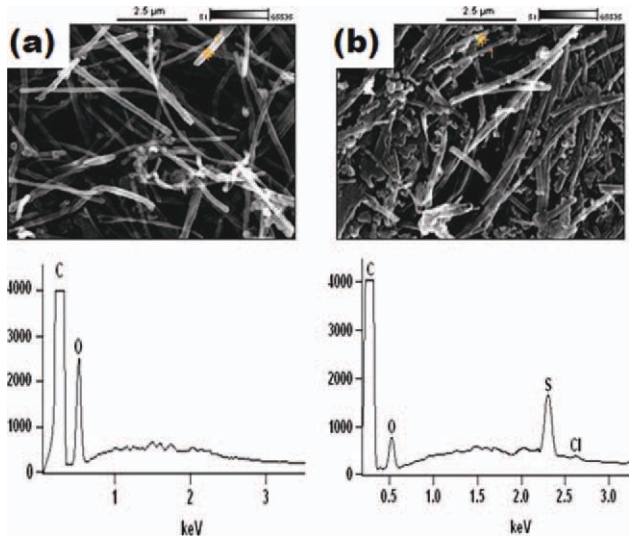

Figure 7 EDX spectra of (a) pristine MWNTs and (b) s-MWNTs. [Color figure can be viewed in the online issue, which is available at wileyonlinelibrary.com.]

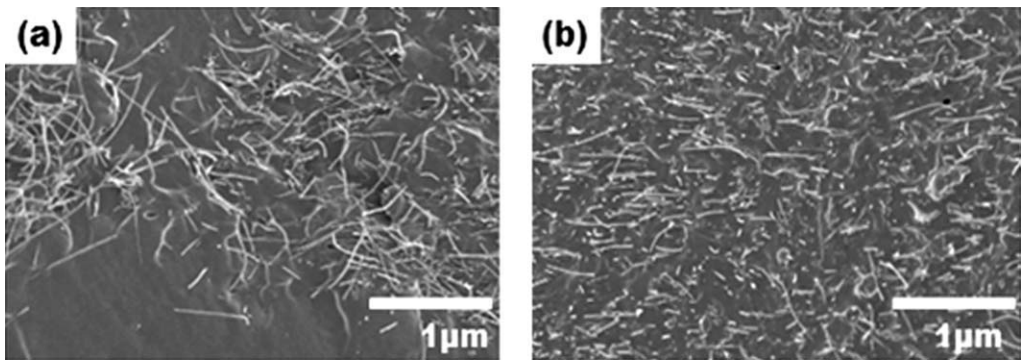

Figure 8 SEM images of (a) pure MWNTs/PES membranes and (b) SPES membranes.

that the surface of the s-MWNTs was thicker and rougher than that of the pure MWNTs.

Energy-dispersive X-ray spectroscopy (EDX) confirmed the existence of sulfonic acid groups on the surface of the s-MWNTs. The spectrum of s-MWNTs [Fig. 7(b)] shows an additional sulfur peak, whereas the spectrum of the pristine MWNTs showed only carbon and oxygen, as shown in Figure 7(a). This suggests that aminomethanesulfonic acid had been introduced successfully onto the surface of the MWNTs.

The distribution of MWNTs in the PES matrix showed a remarkable difference between pure MWNTs [Fig. 8(a)] and s-MWNTs [Fig. 8(b)]. As shown in Figure 8(a), the pure MWNTs were partially aggregated, whereas the s-MWNTs were dispersed homogeneously throughout the entire PES matrix. This phenomenon can be explained in terms of the improved interfacial interaction between the s-MWNTs and the PES matrix. The carboxyl groups remaining on the s-MWNTs surface formed hydrogen bonds with the sulfonic groups of the PES matrix. This resulted in an improved interaction between the s-MWNTs and PES, which prevented aggregation.[39]

Thermal analysis of the SPES membranes

The thermal stability of a PEM is a key property for its durability during fuel cell operation at high temperatures. The thermal stability of the SPES membranes was examined by TGA. Figure 9 shows the two steps of the TGA thermal graph of the SPES membrane with various s-MWNT contents. The first step occurred at approximately 100°C due to the loss of water absorbed by sulfonic acid groups. The second thermal degradation at approximately 300°C is believed to be associated with the sulfonic acid group. The third step of weight loss was associated with the deposition of the PES polymer main chain. For SPES (0%), the onset of the third step of weight loss began at approximately 480°C, but for SPES (3%) and SPES (5%), the onset of the third step of weight loss occurred later, at approximately 500°C. The weight loss of SPESs both 3% and 5% tended to increase with increasing amounts of s-MWNTs introduced into the polymer matrix.[38] In general, hydrogen bonds can increase the thermal stability. As mentioned previously, s-MWNTs could form hydrogen bonds between the carboxyl groups of s-MWNTs and sulfonic group of s-PES. Therefore, the SPES (3% and 5%) membrane should show higher thermal stability than SPES (0%).[38] PES is an excellent thermostable polymer that decomposes at high temperatures (~ 500°C). Therefore, no other additional loss for the SPES membrane was observed at 600°C. From these results, the SPES membranes were still stable enough to serve as PEMs for DMFC applications.

Mechanical property

Table I shows the tensile strength data for PES and SPES membranes with different s-MWNT loadings. (The data in Table I are average values.) The tensile strength of the SPES membranes ranged from 61 to

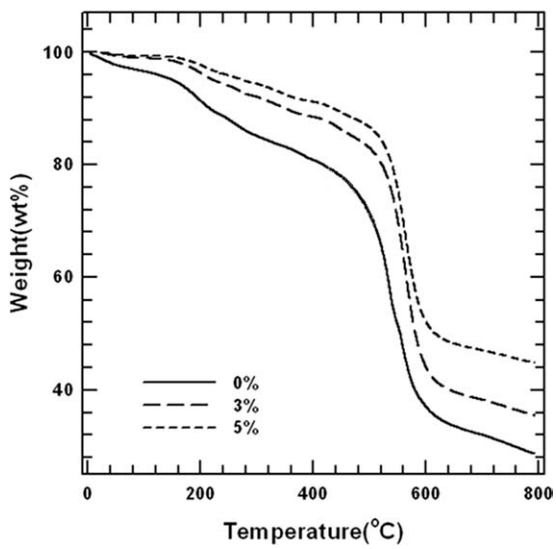

Figure 9 The thermal analysis of the TGA curve.

TABLE I
Mechanical Property of SPES Membranes

s-MWNT concentration (wt %)	C_A[a] (%)	C_B[b] (%)	Methanol permeability (cm^2/s)
Nafion	–	–	2.91×10^{-6}
0 wt %	0.0052	22.23	4.53×10^{-10}
1 wt %	0.0059	24.00	5.27×10^{-10}
2 wt %	0.0090	27.31	7.01×10^{-10}
3 wt %	0.0109	28.12	8.22×10^{-10}
5 wt %	0.0128	29.54	9.19×10^{-10}

[a] C_A = this concentration of methanol in the donor reservoirs.
[b] C_B^2 = this concentration of methanol in the receptor reservoirs.

65.1 MPa. The tensile strength of pure PES membrane was 66 MPa. The decreased tensile strength of s-PES than pure PES is attributed the sulfonation of PES. However, the tensile strength of s-PES/s-MWNTs membrane increased by increasing contents of s-MWNTs. These increased mechanical properties of SPES membranes were affected by the strong interaction that the carboxyl groups remaining on the s-MWNTs surface formed hydrogen bonds with the sulfonic groups of the PES matrix. That is, the improved mechanical strength data is attributed to increased adhesion between filler and matrix and homogeneous dispersion of modified MWNTs in the s-PES matrix. As a result, the s-PES membrane appeared to have good mechanical properties due to the functionalized MWNT reinforced PES systems.

Water uptake

Figure 10 shows the water uptake of various SPES membranes at 25°C, 60°C, and 80°C. The water uptake is related to the proton conductivity, mechanical properties, and dimensional stability. Water can help conduct protons but a high water uptake can weaken the mechanical properties of the membranes. As shown in Figure 10, the water uptake of the SPES membranes increased with increasing s-MWNTs concentration.

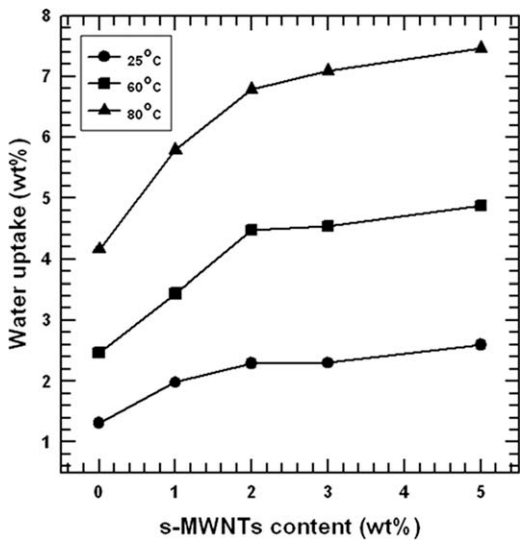

Figure 10 Water uptake of SPES membranes (at 25°C, 60°C, and 80°C).

The amount of water uptake in the sulfonated polymers will be strongly dependent on the amount of sulfonic acid groups. Therefore, the increase in water content was attributed to the strong hydrogen bonding between the water molecules and sulfonic groups (—SO_3H) of the s-MWNT.[23] Another reason is that the carbonyl group of s-MWNTs also forms a hydrogen bond with water molecules. The additional water molecules are preferentially associated with previously absorbed water molecules, which are the hydrogen bonded water molecules.[41]

Note that the water uptake of SPES membranes, which changed from approximately 1.1% at 25°C to 7.2% at 80°C, was slightly lower than that of Nafion® 117.[39]

Methanol permeability and proton conductivity

The proton conductivity of the SPES membranes was measured at temperatures ranging from 25°C to 80°C. Figure 11 shows that a higher proton conductivity leads to a higher power density of the DMFC. The proton conductivity of the SPES membrane ranged from 2.0701×10^{-4} to 7.0788×10^{-3} S/cm at 80°C.

When s-MWNTs were added to the SPES membrane, the proton conductivity of the membranes increased gradually with increasing s-MWNT content. This can be explained by the increase in water absorption (the water uptake of SPES increased with increasing s-MWNTs concentration). The free volume of membranes and the increased motion of

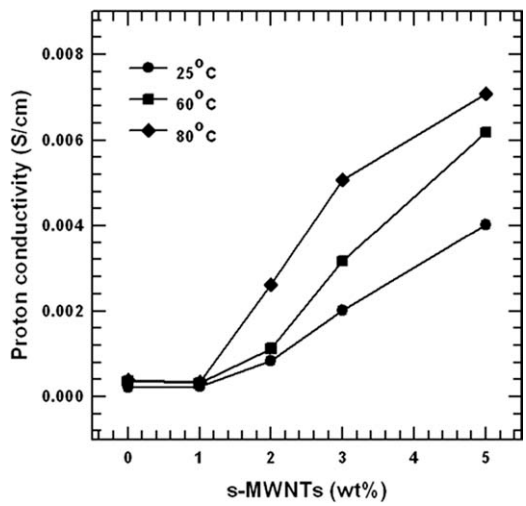

Figure 11 Proton conductivity of SPES membranes.

TABLE II
Methanol Permeability of SPES Membranes

s-MWNTs contents (wt %)	Tensile strength (MPa)
Pure PES	66
0% (s-PES)	61
1%	62.3
3%	64.7
5%	65.1

water and protons led to an increase in the proton conductivity of SPES.[40] As a result, the proton conductivity of the membrane increased with increasing s-MWNT content. These results were also affected by temperature. The 5% SPES membrane increased from 3.9281×10^{-4} S/cm (25°C) to 7.0788×10^{-3} S/cm (80°C).

The water uptake values increased with increasing amounts of s-MWNTs. The proton conductivity of a DMFC membrane relies on its water content. According to the Grotthus mechanism, stationary water molecules help to increase the hopping of protons.[42]

The increase in IEC values suggests that the increase in sulfuric acid groups from the addition of s-MWNTs in the SPES membrane can improve the density of conducting protons at the limited domain. As a result, the SPES membranes have excellent proton conductivity due to both the number of protonated sites (SO_3H) and the formation of water mediated pathways for protons.

In general, inorganic fillers reduce the methanol permeability. The SPES membranes possessed excellent methanol resistance, as shown in Table II. These values were determined from the concentration C_B (the concentration of the MeOH receptor) as a function of time because this factor shows a similar trend to that of permeability. The membrane of the DMFC can use high methanol concentrations at low methanol permeability. As a result, a low methanol permeability results in excellent effective energy density in the DMFC system.[16] The methanol permeability of the SPES membranes (0–5 wt %) ranged from 4.4405×10^{-10} to 9.1008e−10 $cm^2\ s^{-1}$, which were remarkably lower than that of Nafion® 117.[39]

The SPES membranes offered slightly lower proton conductivity and much lower methanol permeability than Nafion® 117.

CONCLUSIONS

Composite membranes of sulfonated MWNTs (s-MWNTs)/sulfonated PES(s-PES) (SPES) with various compositions were prepared using a solution casting method. An interaction force formed between the s-MWNTs and s-PES matrix because the PES matrix has a molecular interaction with the hydroxyl groups of s-MWNTs. Consequently, the dispersion of s-MWNTs in the s-PES matrix produced SPES membranes with a better morphology than the pure MWNTs/s-PES composite membranes. The proton conductivity of the SPES membranes increased with increasing s-MWNTs content in the SPES membranes, and the water adsorption also increased because high IEC values can improve the quantity of sulfonic acid groups. The SPES membranes showed higher proton conductivity (from 3.9281×10^{-4} to 7.0788×10^{-3} S/cm at 80°C) and methanol permeability from 4.4405×10^{-10} to 9.1008×10^{-10} $cm^2\ s^{-1}$ compared with the values reported previously for PES/inorganic membranes and commercial Nafion®.

References

1. Zhao, C.; Lin, H.; Na, H. Int J Hydrogen Energy 2010, 35, 2176.
2. Li, H.; Zhang, G.; Wu, J.; Zhao, C.; Zhang, Y.; Shao, K.; Han, M.; Lin, H.; Zhu, J.; Na, H. J Power Sources 2010, 195, 6443.
3. Higa, M.; Sugita, M.; Maesowa, S.; Endo, N. Electrochem Acta 2010, 55, 1445.
4. Yang, C.; Lee, Y.; Yang, J. M. J Power Sources 2010, 188, 30.
5. Yang, T. Int J Hydrogen Energy 2009, 34, 6917.
6. Kim, D. S.; Cho, H. I.; Kim, D. H.; Lee, B. S.; Yoon, S. W.; Kim, Y. S.; Moon, G. Y.; Byun, H. S.; Rhim, J. W. J Memb Sci 2009, 342, 138.
7. Wang, E. D.; Zhao, T. S.; Yang, W. W. Int J Hydrogen Energy 2010, 35, 2183.
8. Kim, D. S.; Park, H. B.; Rhim, J. W.; Lee, Y. M. J Memb Sci 2004, 240, 37.
9. Yang, T. J Memb Sci 2009, 342, 221.
10. Min, S. H.; Kim, D. J. Solid State Ionics 2010, 180, 1690.
11. Huang, C. H.; Wu, H. M.; Chen, C. C.; Wang, C. W.; Kuo, P. L. J Memb Sci 2010, 353, 1.
12. Yang, C. C.; Chiua, S. J.; Leea, K. T.; Chiena, W. C.; Lina, C. T.; Huang, C. A. J Power Sources 2008, 184, 44.
13. Xiong, Y.; Liu, Q. L.; Zhang, Q. G.; Zhu, A. M. J Power Sources 2008, 183, 447.
14. Yang, C. C.; Chiu, S. J.; Chien, W. C. J Power Sources 2006, 162, 21.
15. Balbas, M.; Gozutok, B. Synth Met 2010, 160, 150.
16. Zhou, S.; Kim, J. E.; Kim, D. J. J Memb Sci 2010, 348, 319.
17. Seo, D. W.; Lim, Y. D.; Lee, S. H.; Jeong, Y. G.; Hong, T. W.; Kim, W. G. Int J Hydrogen Energy 2010, 35, 13088.
18. Oh, Y. S.; Lee, H. J.; Yoo, M. J.; Kim, H. J.; Han, J. H.; Kim, T. H. J Memb Sci 2008, 323, 309.
19. Wen, S.; Gong, C.; Tsen, W. C.; Shu, Y. C.; Tsai, F. C. J Appl Polym Sci 2010, 116, 1491.
20. Kwon, Y. H.; Kim, S. C.; Lee, S. Y. Macromolecules 2009, 42, 5244.
21. Shu, Y. C.; Chuang, F. S.; Tsen, W. C.; Chow, J. D.; Gong, C.; Wen, S. J Appl Polym Sci 2008, 107, 2963.
22. Prashantha, K.; Park, S. G. J Appl Polym Sci 2005, 98, 1875.
23. Wen, S.; Gong, C.; Tsen, W. C.; Shu, Y. C.; Tsai, F. C. Int J Hydrogen Energy 2009, 34, 8982.
24. Meng, H.; Sui, G. Z.; Fang, P. F.; Yang, R. Polymer 49, 2008, 610.
25. Bokoza, S. Polymer 2007, 48, 4907.
26. Yang, K.; Gu, M.; Guo, Y.; Pan, X.; Mu, G. Carbon 2009, 47, 1723.

27. Iijima, S. Nature 1991, 354, 56.
28. Li, F.; Cheng, H. M.; Bai, S.; Su, G.; Dresselhaus, M. S. Appl Phys Lett 2000, 77, 3161.
29. Zhao, X.; Bryan, T.; Chu, T.; Ballesteros, B.; Wang, W.; Jonston, C.; John, M. S.; Patrick, S. G. Nanotechnology 2009, 20, 9.
30. Chen, X.; Chen, X.; Lin, M.; Zhong, W.; Chen, X.; Chen, Z. Macromol Chem Phys 2007, 208, 964.
31. Kuan, H. C.; Ma, C. C.; Chang, W. P.; Yuen, S. M.; Wu, H. H.; Lee, T. M. Comput Sci Technol 2005, 65, 1703.
32. Joo, S. H.; Pak, C. H.; Kim, E. A.; Lee, Y. H.; Chang, H.; Seung, D. Y.; Choi, Y. S.; Pak, J. B.; Kim, T. K. J Power Sources 2008, 180, 63.
33. Thomassin, J. M.; Kollar, J.; Caldarella, G.; Germain, A.; Jérômea, R.; Detrembleur, C. J Memb Sci 2007, 303, 252.
34. Ma, C.; Zhang, W.; Zhu, Y.; Ji, L.; Zhang, R.; Koratkar, N.; Liang, J. Carbon 2008, 46, 706.
35. Sharma, A.; Kumar, S.; Tripathi, B.; Singh, M.; Vijay, Y. K. Int J Hydrogen Energy 2009, 34, 3977.
36. Li, L.; Wang, Y. J Memb Sci 2005, 246, 167.
37. Shahi, V. K. Solid State Ionics 2007, 177, 3395.
38. Guan, R.; Zou, H.; Lu, D.; Gong, C.; Liu, Y. Eur Polym J 2005, 41, 1554.
39. Striolo, A.; Chialvo, A. A.; Cummings, P. T.; Gubbins, K. E. J Chem Phys 2006, 124, 072710.
40. Zhong, S.; Cui, X.; Fu, T.; Na, H. J Power Sources 2008, 180, 23.
41. Zhou, S.; Wu, Q.; Liu, Z. Polym Bull 2006, 56, 95.
42. Sundar, S.; Jang, W.; Lee, C.; Shul, Y.; Han, H. J Polym Sci Part B: Polym Phys 2005, 43, 2370.